27th EPS Conference on Contr. Fusion and Plasma Phys. Budapest, 12-16 June 2000 ECA Vol. **24B** (2000) 1473 -1476

Bulk, Peripheral and Near Antenna rf Power Absorption in Highly Collisional Helicon Plasma

K. P. Shamrai[1], S. Shinohara[2] and V. A. Yavorskij[1]

[1] *Institute for Nuclear Research, 47 prospect Nauki, Kiev 03680, Ukraine*
[2] *Interdis. Grad. Sch. Eng. Sci., Kyushu University, Kasuga, Fukuoka 816-8580, Japan*

The operation of helicon plasma source has normally being examined in the area of relatively low gas pressures where the electron collision frequency ν_e is less or about ω, the driving frequency (see [1, 2] and references therein). Helicon discharge demonstrates in this area a complicated behavior including abrupt density jumps. At high pressures, of order a few tens mTorr, the electron collision frequency is higher, or even much higher than ω. As long as helicons may be low damping and propagating waves even at $\nu_e \gg \omega$, they can support an efficient discharge in this area. However, little experimental data are available so far on helicon plasmas at high pressures.

In recent experiments [3], detailed measurements were conducted on the operation modes of high pressure helicon discharge. The jump to the high density mode, in the range of 10^{13} cm^{-3}, occurs in this discharge as well as in low pressure one. Density jump is accompanied by the jump of the plasma load resistance, and by substantial alteration of the rf magnetic field profiles. The goal of this report is to compare with theory the experimental data from high pressure source (for more details see [4]). To estimate the effects of the bulk vs peripheral and under antenna vs downstream absorption, we computed profiles of the rf power absorption and partition of absorbed power between various spatial areas in plasma.

Experiments were performed with a source excited by double $m = 0$ antenna at frequency 7 MHz and Ar pressures up to 51 mTorr [3,4]. Depending on the electron density and temperature, ν_e/ω made the value of 10 and higher. Data were taken in a wide range of input power and magnetic field, and with parallel or anti-parallel currents in the antenna loops. Transition of the discharge into the high density mode happens at threshold power of 100 to 1000 W, depending on conditions, and gives rise to abrupt increase of the plasma load resistance and to much deeper penetration of wave fields into the downstream plasma.

Computations have been conducted using generalized model [5], with plasma nonuniformity included, and Mathematica 3.0. The source is modelled by a cylindrical plasma column, of radius $r_0 = 2.5$ cm and length $\Delta z = 160$ cm, with two conducting flanges at $z = \pm 80$ cm. Two loops of the $m = 0$ antenna, of radius $r_a = 3$ cm and width $d = 1$ cm, and with a 1 cm split between them, are centered at $z_a = -20$ cm, and contain equal in amplitude currents of either parallel or anti-parallel directions. The antenna current density and fields are expanded into Fourier series over axial wavenumbers $k = l_z\pi/\Delta z$ ($l_z = 1, 2,...$). Cold plasma permittivity tensor includes electron-neutral and electron-ion collisions, and ion collisions. Landau damping is negligible at high pressures [4]. Parabolic density profile, $n = n_0 - (n_0 - n_{edge})(r/r_0)^2$, is used with the edge density n_{edge} ranging 0 to the central value n_0. However, the effect of nonuniformity turns out to be not so dramatic for the $m = 0$ excitation, as it is for the $m = \pm 1$ antennas [6,7]. As well, the profile is much more uniform at high collisions as compared to low collisions. All the data are presented below for the argon pressure of 51 mTorr.

Computed plasma resistance is found to be low sensitive to the electron temperature, and thus to the electron collision frequency. In contrast with low collisions [5], the variation of resistance with density is quite smooth: absorption maxima and minima are blurred out (see Fig. 1). For the same reason, the resistance does not demonstrate any peculiarities in the range of magnetic fields relative to the lower hybrid resonance. Integral characteristics, like the total

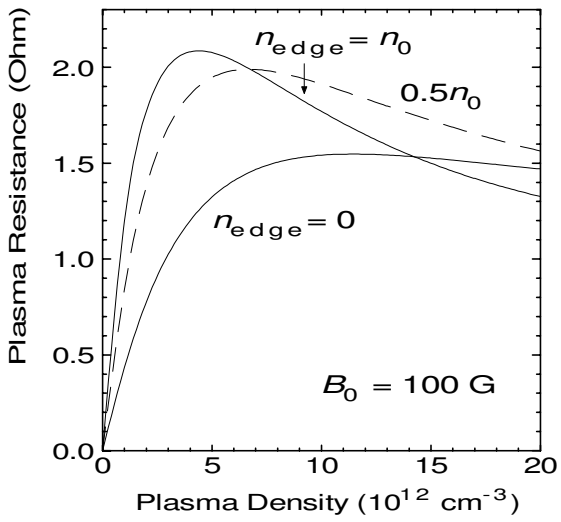

Fig. 1. Dependences of plasma resistance on central density n_0, at various edge densities.

absorbed power and thus the plasma resistance, are sensitive to the degree of plasma nonuniformity at low densities only, but do not show strong variation at high densities, as seen from Fig. 1.

Fig. 2 compares experimental and computed profiles of the axial magnetic field at the plasma center with anti-parallel excitation. The measured density profile is quite uniform in this case, so that the uniform model used in computation yields a quite good agreement. A disagreement that is seen at high density to the left from antenna is thought to arise from distortions induced by magnetic probe.

Computed and measured dependences of the plasma resistance on density and on input power are shown in Fig. 3, for B_0 = 100 G. Theoretical threshold for jump, n_{th}, was estimated using the power balance consideration [8,9]. In computation, nonuniform plasma profile with $n_{edge} = n_0/2$ was used for the parallel antenna currents, and the uniform approximation for anti-parallel currents. In both cases the agreement seems to be satisfactory.

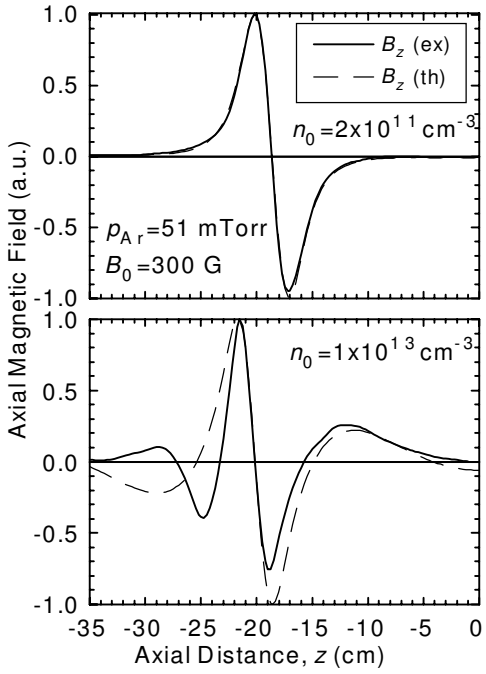

Fig. 2. Measured and computed profiles of B_z before (top) and after (bottom) the jump, for the anti-parallel antenna currents.

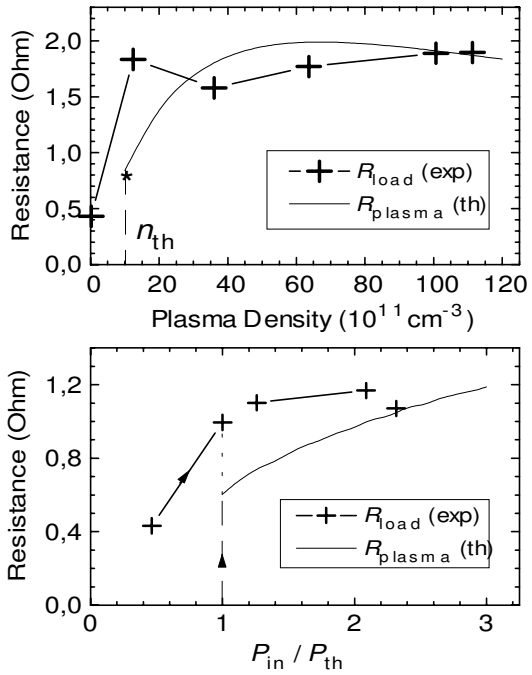

Fig. 3. Loading resistance vs density, for parallel currents (top), and vs input power, for anti-parallel currents (bottom).

Fig. 4 shows specific absorbed power, $\log_{10}(p_{abs})$ with p_{abs} in mW/cm^3, computed for uniform profiles with $n_0 = 2\times10^{12}$ and 2×10^{13} cm^{-3}, at parallel currents. (The antenna current for Figs. 4-6 is equal 1 A). With increasing density, damping of helicons increases and so the absorption profile is shrinking in axial direction. The increase of a peripheral absorption with

density is due to the surface mode conversion of helicons into Trivelpiece-Gould (TG) waves, which arises from the polarization induced by helicons at abrupt edge [5]. A strong near-antenna peak is formed jointly by short evanescenting helicon modes and TG waves. At anti-parallel antenna currents, the picture of absorption differs substantially: absorption profile with increasing density is spreading from the antenna, both axially and radially. In this case, antenna produces short modes which can penetrate deeply into plasma at high densities only.

The change of absorption (in log scale) with magnetic field is shown in Fig. 5, for parallel antenna currents and uniform density $n_0 = 2\times10^{13}$ cm^{-3}. In combination with bottom figure 4, this figure shows that increasing magnetic field results in spreading of the absorption profile in all the directions, and in increasing of the peripheral absorption via TG waves.

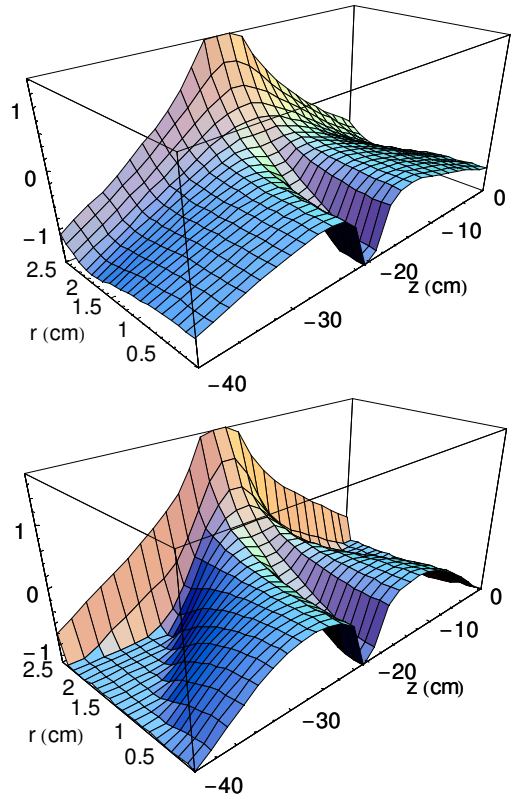

Fig. 4. Absorption profiles at low (top) and high (bottom) densities. $B_0 = 300$ G.

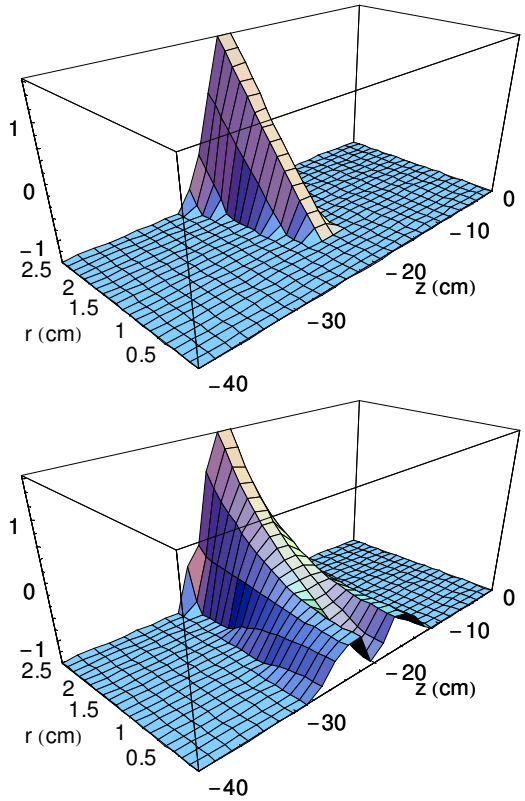

Fig. 5. Absorption profiles at high density for $B_0 = 0$ G (top) and 100 G (bottom).

Fig. 6 shows the effect of plasma nonuniformity on the absorption profile (log scale), at fixed central density of $n_0 = 2\times10^{13}$ cm^{-3} and $B_0 = 300$ G. By comparing these plots and that in bottom figure 4, one can see that substantial changes occur if the edge density is low enough. The decrease of the edge density results in reducing of the peripheral absorption via surface mode conversion. This reduction, however, is substantially compensated by increasing absorption due to the bulk conversion of helicons into TG waves. (The latter results from the bulk plasma polarization in helicon fields, and increases at higher ∇n [9].) That compensation is the reason for that why the plasma resistance is varying with nonuniformity only slightly, as seen from Fig. 1. For lower edge density, absorption profile becomes wider in axial direction owing to both a deeper penetration of helicons into bulk plasma and to the bulk conversion.

To estimate the space partition of absorption, an axial part of the column centered at the antenna ($|z - z_a| < 2$ cm) was considered as the near antenna region, and a radial layer near

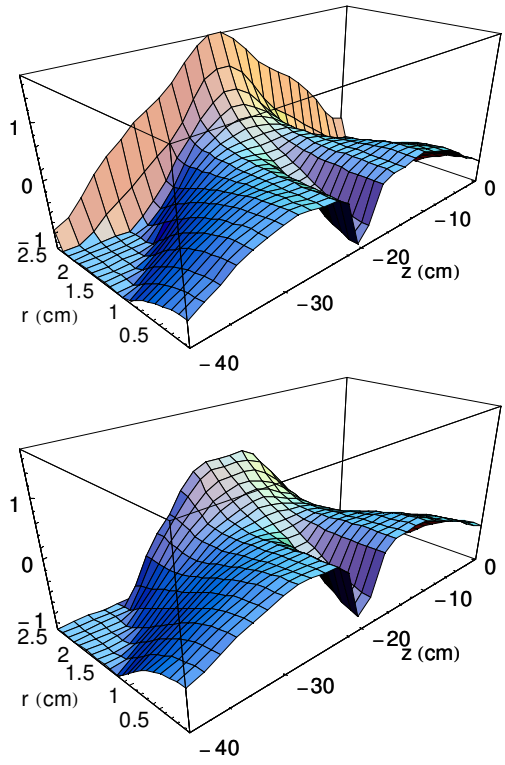

Fig. 6. Absorption profiles in nonuniform plasma. $n_{edge} = 0.5n_0$ (top) and 0 (bottom).

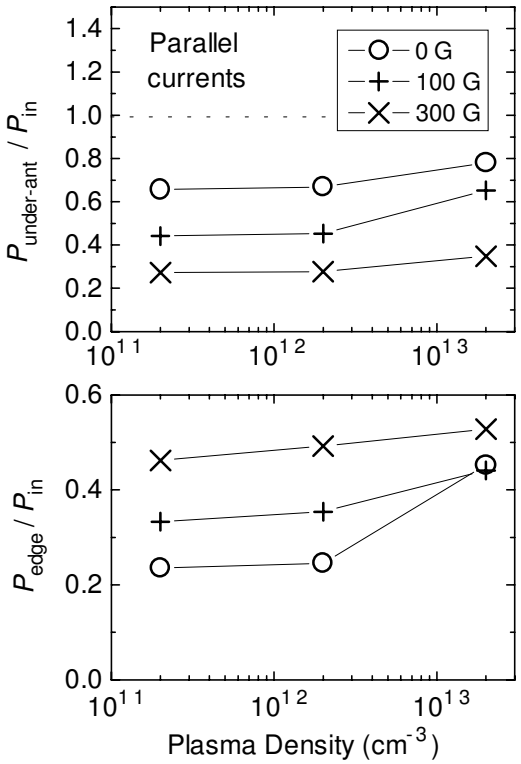

Fig. 7. Power fractions absorbed in near antenna (top) and edge (bottom) regions.

the plasma boundary ($r_0 - r < 0.2$ cm), which makes approximately 15% of the total volume, as the edge region. Fractions of the total power absorbed in these regions were computed at various densities and magnetic fields and are shown in Fig. 7, for parallel antenna currents and $n_{edge} = n_0/2$. One can see that near antenna absorption drops while edge absorption increases with magnetic field. Both change considerably with density above 10^{12} cm^{-3}.

In conclusion, various data from the high pressure helicon source, including the field profiles, variation of load resistance with density and input power, and thresholds for density jumps, are satisfactorily fitted with computation results. Computations yield the plasma resistance to be low sensitive to the plasma nonuniformity at high densities. Computed absorption profiles show that substantial fractions of power are deposited axially in short near antenna region, and radially in narrow near edge region. These fractions depend only slightly on the central plasma density and on the edge density, if the latter is not very low, but substantially depend on the magnetic field and antenna spectrum (parallel or anti-parallel antenna currents). The shape of absorption profile does not change substantially with density, below 10^{12} cm^{-3}, and, except for the edge region, with the degree of plasma nonuniformity.

[1] Boswell R W and Chen F F 1997 *IEEE Trans. Plasma Sci.* **25** 1229
[2] Chen F F and Boswell R W 1997 *IEEE Trans. Plasma Sci.* **25** 1245
[3] Shinohara S and Yonekura K 2000 *Plasma Phys. Control. Fusion* **42** 41
[4] Shinohara S and Shamrai K P 2000 *Plasma Phys. Control. Fusion* **42** (to be published)
[5] Shamrai K P, Pavlenko V P and Taranov V B 1997 *Plasma Phys. Control. Fusion* **39** 505
[6] Arnush D and Chen F F 1998 *Phys. Plasmas* **5** 1239
[7] Krämer M 1999 *Phys. Plasmas* **6** 1052
[8] Lieberman M A and Lichtenberg A J 1994 *Principles of Plasma Discharges and Materials Processing* (New York: Wiley)
[9] Shamrai K P 1998 *Plasma Sources Sci. Technol.* **7** 499